The atmosphere of a sunspot based on observations in the x-ray, extreme ultraviolet, optical, and radio ranges

J. Staude, F. Fürstenberg, J. Hildebrandt, A. Krüger, J. Jakimiec, V. N. Obridko, M. Siarkowski, B. Sylwester, and J. Sylwester

Central Institute for Solar-Terrestrial Physics, Berlin, GDR, Astronomical Observatory of Wroclaw University, Wroclaw, Poland, and Institute of Terrestrial Magnetism, the Ionosphere, and Radio-Wave Propagation, USSR Academy of Sciences

(Submitted May 23, 1983)

Astron. Zh. **61**, 956–967 (September–October 1984)

It is shown that the lower chromosphere of an umbra is best described within the framework of a model close to that of Teplitskaya *et al*. This model can be extended to higher levels using a large temperature gradient, so that $T \approx 40{,}000$ K and an electron density $n_e \approx 4 \cdot 10^{10}$ cm^{-3} are reached at a height $z \approx 2000$ km above the umbral photosphere. These values are defined by the EUV data of the HRTS instrument. At higher levels one must presume the existence of at least two components: The hot component, which occupies $\alpha \approx 0.8$–0.9 of the total volume, has a narrow transition layer, and the coronal values of $T \approx 1.8 \cdot 10^6$ K and $n_e \approx 5 \cdot 10^8$ even at a height $z = 3000$–5000 km. These values are consistent both with the absence of an x-ray emission flux above large sunspots and with the high brightness temperature $T_b = 1.8 \cdot 10^6$ K of emission in the centimeter range from the same region. This hot coronal matter surrounds the bases of cool loops emerging from the umbra in the form of bundles, and they emit the EUV lines observed at $10^4 \leq T \leq 10^6$ K. In the corona the z dependence of all the physical quantities, including α, over a distance of several thousand kilometers can be taken as weak. Along the axis of a loop T grows slowly, the loops become more horizontal, and at distances and heights of several tens of thousands of kilometers above a flocculus they appear as hot x-ray loops.

1. INTRODUCTION

A working conference on active regions (AR) on the sun, which was held at the Astronomical Institute of Wroclaw University (Poland) from November 28 to December 6, 1979, is summarized in the present article. At the conference a small group of solar physicists from several observatories took up the discussion of possible interpretations of the observed emission from a sunspot umbra, from the region above the umbra, in different wavelength ranges. The preliminary results were given at two conferences.[1,2] This work was continued at a working conference at the Astronomical Observatory of Ondřejov (Czechoslovakia) from September 28 to October 3, 1981. Some of the main results of these meetings are summarized here, while we intend to publish more detailed calculations separately (also see Ref. 3).

In 1966 Livshits, Obridko, and Pikel'ner[4] proposed a model of the atmospheric layers above sunspots which assumes that the transition layer starts in the umbral chromosphere at a height z of about 2000 km above the photosphere and approaches coronal values of the electron temperature, T > 10^6°K, at heights of $\sim 3 \cdot 10^3$ km. This model could explain the observed microwave spectrum of the S component of sunspots by the fact that gyromagnetic emission in a strong magnetic field makes the main contribution to the emission. New observational data subsequently appeared, including data with a high spatial resolution in the x-ray and extreme ultraviolet ranges, obtained on Skylab[5–10] and the High Resolution Telescope and Spectrograph (HRTS),[11–13] as well as data in the centimeter radio range, obtained during a solar eclipse.[14] It soon became clear that these data cannot be explained simultaneously within the framework of a homogeneous model with plane-parallel stratification of the atmosphere above the umbra. Therefore, Obridko[15] proposed a new two-component model consisting of cool and hot elements (loops), with the fraction of the cool elements decreasing with height. This model made it possible to eliminate the majority of the difficulties arising in attempts to interpret the observations in the various wavelength ranges within the framework of a homogeneous model. Even it required refinements, however, after results were published on new observations of large sunspot groups in the x-ray and centimeter ranges,[16] eliciting a lively discussion. It is especially difficult to make more precise the relative fractions of the hot and cool elements and the height dependdence of these fractions. New observations of x-ray and EUV emission with a high resolution (see Ref. 17) and data on radio sources have recently appeared, a comparison with which permits one more test of the model proposed by the authors.

In the following sections, on the basis of observational data, we shall determine the demands imposed on the model and describe the proposed concept, as well as present the first detailed calculations of the emission in the different wavelength ranges on the basis of this model. Finally, statements are made about the further improvement and expansion of the model in the future.

2. MODEL OF AN UMBRA AT THE PHOTOSPHERIC AND CHROMOSPHERIC LEVELS

Reliable empirical models of the atmosphere in the umbra of a sunspot at the photospheric level exist, based on observations in the infrared and visible regions of the spectrum. At greater heights, starting with the temperature minimum, the uncertainty grows. From now on we shall try to use only observational data from the cited papers. All the model calculations are made anew, particularly the conversion of the various height scales (the geometrical depth z, the optical depths in the continuum at $\lambda_0 = 5000$ Å $[\tau_0]$ and at other wavelengths λ $[\tau_\lambda]$, the scale of mass m, etc.). Such an approach allowed us to obtain a rather self-consistent model with identical assumptions about the chemical composition and the methods of solving

 0038-5301/84/05 0557-07 $04.10

the equations of state, the hydrostatic equilibrium in the atmospheric layers, departures from local thermodynamic equilibrium, the absorption coefficients, etc., but slight differences are possible in a comparison with the original models, of course. The values of the temperature $T(\tau_0)$ and electron pressure $p_e(\tau_0)$ in the photospheric layers were taken from the sunspot model of Stellmacher and Wiehr.[18] For the lower chromosphere we constructed various models of sunspots based on observations in moderately strong lines, in Hα, and especially in Ca II H and K (Refs. 19-23). Observational data in the extreme ultraviolet region with a high spatial resolution of $\lesssim 1''$ were recently obtained.[12,13,24-28] These data were used to test and expand the existing chromospheric models in order to obtain a working model of a sunspot umbra up to $T \lesssim 40{,}000$°K. It was found that the trend of T(z) for $\lesssim 11{,}000$°K in the model of Teplitskaya et al.[21,22] agrees best with the new data, whereas the values of p_e adopted by us are somewhat overstated. (We assumed hydrostatic equilibrium with a total pressure $p = p_g + p_{tu}$, assuming $p_{tu} = \rho v^2/2$, where p_{tu} is the turbulent pressure, ρ is the density, and v is the turbulent velocity, whereas in Refs. 21 and 22 the electron density $n_e = p_e/kT$ was found directly from the observations, without the assumption of hydrostatic equilibrium; k is the Boltzmann constant.)

Extension of the model toward higher values of z and T leads to an increase in the gradient T(z), which exceeds at least twofold the value of the gradient in facular points and is considerably larger than for the undisturbed sun. The values of the electron density n_e at different temperatures prove to lie between the values in facular points and in bright points of the network in the quiet chromosphere.

The models of the average undisturbed photosphere and the chromosphere were taken from Refs. 29 and 13, while the extension of both models to subphotospheric layers was obtained earlier using model calculations and discussions, are presented in Fig. 1. Here the zero point of the z scale is chosen so that the Wilson depression, equal to 700 km, is taken into account (z = 0 at $\tau_0 = 1$ in the umbra, z = 700 km at $\tau_0 = 1$ in the undisturbed photosphere). Then the densities in the two models coincide at z = 0 in accordance with Ref. 32. This part of the model calculations is described in more detail in Ref. 33, while a preliminary variant of the models has already been used in Staude's paper.[34] Analogous model calculations were also made later for a model of a facula and for several variants of umbra models, which differ in their extent in height and hence have different electron densities n_e and gradients of temperature T (see Ref. 35 for the concrete characteristics of these models). Various models of v(z) were also tried. Complete quantitative tables of these models are published in Ref. 36, where the computer calculation programs are also described.

A complete model of the chromosphere above a sunspot was recently developed by Lites and Skumanich.[37] This model will be designated below as LS. The height dependence of the temperature, T(z), in the LS model was used by Avrett[38] to calculate the standard model atmosphere (sunspot model). In Fig. 1 our model is compared with the LS model. It is seen from Fig. 1a that the T(z) relations are close in the two models. Certain differences are connected with the hypothesis of two temperature

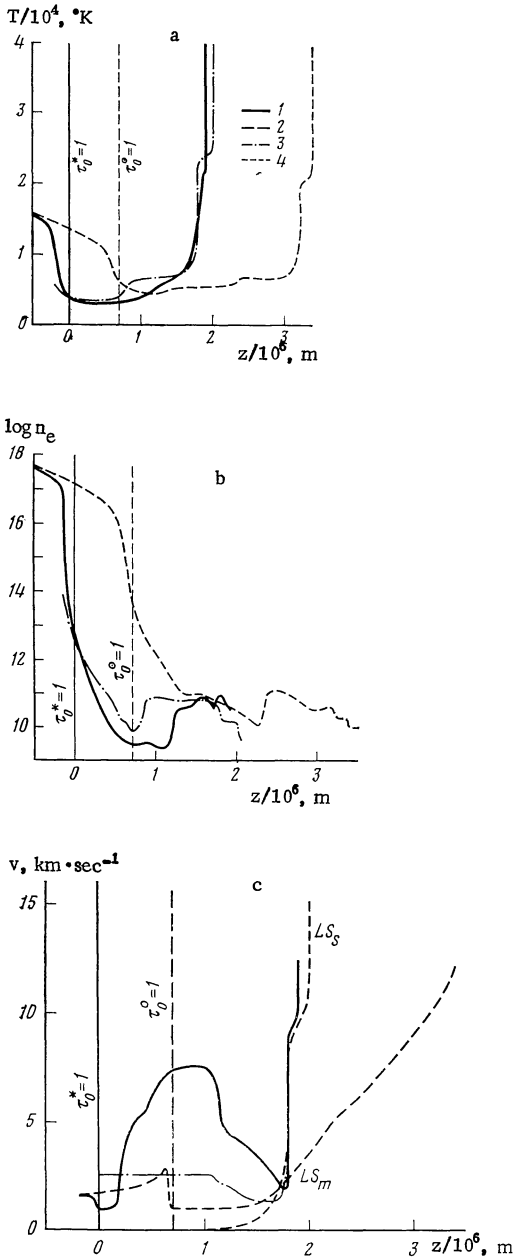

FIG. 1. Temperature, $T \cdot 10^{4}$°K (a), electron density n_e, cm^{-3} (b), and turbulent velocity v (c) as functions of the geometrical height z in the adopted sunspot model (1), the model of the average undisturbed sun (2), and the LS model (3). In c in the LS model, besides the microturbulent velocity v, the systematic velocity is given (4), which is not taken into account in calculating the turbulent pressure. The levels of the unit optical depth in the sunspot (τ_0^*) and in the undisturbed atmosphere ($\tau_0^\odot$) are designated in the figure.

plateaus in the LS model, which leads to higher values of T in the lower chromosphere and somewhat lower values of T in the upper chromosphere. The same thing is true correspondingly for n_e (Fig. 1b). The presumed v(z) trend is given in Fig. 1c. Only part of the velocity, designated as LS_m in Fig. 1c, was taken into account for the calculation of p_{tu} in the LS model. The rest of the velocity, which the authors of the LS model took to be the systematic velocity (LS_S), is close to the v(z) trend in the upper chromosphere adopted in our model. In other recent models of the lower chromosphere above a sunspot umbra[39,40] the extent of the chromosphere is far less, so that T and n_e

are larger than in the models discussed above. In one other recent model of the upper chromosphere and corona above a sunspot umbra[41] the values p_e are two to three times higher than in our model and 10 times higher than in the LS model.

3. EXTENSION OF THE MODEL TO THE TRANSITION LAYER AND CORONA

In Ref. 16 the high-resolution x-ray photographs obtained on Skylab (spatial resolution 2", spectral range 2-60 Å) are compared with the data of radio observations obtained on the Stanford interferometer (spatial resolution 16" in one direction) at 2.8 cm. Two peculiarities are noted.

First, as would be expected, increased microwave emission with brightness temperatures of $\sim 2 \cdot 10^5$ °K was observed above facular fields; on the disk these regions coincide with regions of increased x-ray emission. As authors point out, the interpretation of these emissions evidently is not complicated: The x-ray emission comes from hot loops above the facular fields ($T \gtrsim 2.5 \cdot 10^6$ °K, $n_e \approx 10^9$-10^{10} cm^{-3}). These regions are optically thin and they can be neglected in the microwave range, since the magnetic fields are inadequate for the generation of gyromagnetic emission. On the other hand, in thermal bremsstrahlung the main microwave flux arises in deeper layers of the atmosphere, where the temperature is considerably lower. It should be mentioned that data giving evidence of gyroresonance absorption in the tops of the hot loops are presented in Ref. 42. This result was obtained with the help of radio maps at 3.7 and 11 cm with resolutions of 1".5-3".4 and 4".6-10".2, respectively, EUV spectroheliograms, and photographs in x-ray emission. The observed values of $T_b \approx (2.4\text{-}3.0) \cdot 10^6$ °K at the radio-emission maximum agree with the values of T obtained from the x-ray and EUV data. The calculated field strength of B ≈ 300 G at heights of order 10^4 km is comparable with our earlier extrapolations of the force-free magnetic field from data on active regions containing large sunspots.[43,44] There are disagreements about such an interpretation, however: Thus, in Ref. 45, based on data of observations of flocculi at 6 cm using the Very Large Array (VLA) — the intensity I and the circular polarization V — values of $T \approx 2.5 \cdot 10^6$ °K, $n_e \approx 5 \cdot 10^9$ cm^{-3}, and B ≈ 250 G were obtained under the assumption of thermal bremsstrahlung. On the other hand, in Ref. 46 it was shown that gyroresonance absorption at low harmonics (B ≈ 600 G for the third harmonic) is the main mechanism for most of the emission at 6 cm.

Second, the picture has a more complicated character above or near the central parts of large sunspots: Here the maxima of the flux of radio emission with $T_b \approx 1.8 \cdot 10^6$ °K coincide with the minima in x-ray emission, in contrast to what we see above a flocculus. Indications of a decrease in x-ray emission above large sunspots can also be found in other Skylab data.[47] Calculations of the x-ray emission in the spectral range under consideration, made by the Wroclaw group, give an upper limit of $T \lesssim 2 \cdot 10^6$ °K above sunspots, or else x-ray emission should have been observed. The model calculations of Gel'freikh and Lubyshev[48] showed that these values are also comparable with those for high-resolution microwave observations. They adopted a simple model of the corona above a sunspot with $T = 1.8 \cdot 10^6$ °K and $n_e = 2 \cdot 10^{19}$ cm^{-3} at $z = z_t = 2000$ km, where z_t is the height of the transition layer between the chromosphere and corona above $\tau_0 = 1$. The emission from the transition layer (it is assumed that it is infinitely thin) and chromosphere (T = 0) was ignored, the magnetic structure of a sunspot was represented in the form of a dipole, and the expressions for the optical depth of the gyroresonance levels were taken from Zlotnik's paper[49] under the assumption that gyroresonance absorption is the main process responsible for the observed microwave emission in the strong magnetic field of the sunspot umbra. The spectra and the spatial distribution of T_b calculated within the framework of this model are comparable, for the greater part, with the existing observational data. In several cases[16] values of T_b considerably higher than the average value of $T_b = 1.8 \cdot 10^6$ °K have been noted, with individual values fluctuating from $4 \cdot 10^5$ to $4.7 \cdot 10^6$ °K. These higher values cannot be reconciled with a model in which x-ray emission is absent, but the wide range of T_b values is due at least partly to inaccuracies in determining the size of the source (this assumption is supported by strong brief fluctuations in T_b during observations of a single sunspot). Moreover, some of the high values of T_b cited are either connected with sunspots above which the x-ray emission did not disappear or the x-ray data were not published. In a number of recent papers with a high resolution at 6 cm (Refs. 50 and 51) ring-shaped and horseshoe-shaped structures are found on maps of intensity I and circular polarization V, which are consistent with calculations from the model of Gel'freikh and Lubyshev,[48] and in this case they cannot be considered as proof of a strong decrease in T and n_e above the center of the umbra, as is sometimes done erroneously.

The above-described model, intended for the explanation of both the x-ray and the microwave emission, must be made more complicated to explain the high-resolution EUV observations, which are described in Sec. 1 and point to abrupt enhancement of emission lines immediately above the umbra as compared with the surrounding flocculus at temperatures of about $10^4 \lesssim T \lesssim 10^6$ °K. This means that the cool plasma in the loops at the temperatures of the transition layer coexists with the hot corona above the umbra, and our model must thus be expanded so that it includes such inhomogeneous structures. As for the various kinds of emission, our calculations support the following concept. Starting with values of $n_e \approx 4 \cdot 10^{10}$ cm^{-3} and $T \approx 40{,}000$°K at z = 2000 km, characteristic of the middle chromosphere, we have a hot component with an abrupt transition layer and coronal values of $T \approx 1.8 \cdot 10^6$ °K and $n_e \approx 5 \cdot 10^8$ cm^{-3} even at z = 3000-5000 km, occupying a volume $\alpha \approx 0.8$-0.9 and surrounding the bases of the cool loops, which emerge in a bundle from the umbra. The remaining 10-20% of the material of the cool loops permit one, first, to explain the observed emission measure within the limits of the observational errors and, second, to treat the influence of the volume fraction $\beta = 1 - \alpha$ on the resultant radio-emission flux as a dilution factor in the first approximation. In the corona the dependence of all the physical quantities, including α, on z can be considered as insignificant at distances of several thousand kilometers. At the same time, in the horizontal direction, i.e., perpendicular to the magnetic field lines, all the transfer mechanisms are much weakened and very strong T and p_e gradients must actually exist. Along the direc-

tion of the loops T grows slowly. Loops having a larger extent are hotter, evidently, which agrees with the appearance of hot loops at distances and heights of several tens of thousands of kilometers above the facular region. Models of such loops have been discussed, e.g., in Refs. 52 and 53. Cool Hα loops with the inverse Evershed effect, forming a superpenumbra,[54] consist of low-lying structures emerging from the sunspot umbra toward the side at a low chromospheric level ($z \approx 2000$ km).

The proposed model is supported by the most recent sunspot observations in the period of the Solar Maximum Year (SMY). In Ref. 55 a lower limit for the quantity α of $\geqslant 0.7$ was established for the majority of umbras. Cool loops definitely have an unresolved filamentary structure, while hot loops are not envelopes around cooler loops but consist of independent structural elements.[41,56,57] In addition, observations in the SMY period confirmed the values of the parameters adopted in our model: $\log (n_e T/k \cdot \mathrm{cm}^{-3}) \approx 15.0$–$15.3$ in the transition region in the lower corona above an umbra.[58]

The unexpectedly high values of $B \approx 1000$–1400 G based on measurements[59] in a line formed at $T \approx 10^5$ °K point to a deeply placed transition layer at heights on the order of several thousand kilometers. In Ref. 60 it is stated, on the basis of an analysis of projection effects, that the level of formation of the emission at 6 cm above a sunspot is $3.5 \cdot 10^4$ km, which contradicts our assumption that the thin transition layer is deeply situated. However, the field strengths required to explain the observations of I and V gyroresonance emission at the third (second) harmonic are $B \approx 600$ G (900 G). Such a small B gradient contradicts all existing calculations on extrapolation of the field into the chromosphere and corona (see Ref. 61). At a working conference on the SMY in March 1981, F. Chiuder-Drago gave an account of observations of AR 2490 starting with June 10, 1980, including high-resolution radio maps at 2 cm (I – VLA) and 6 cm (I and V – Westerbork Solar Radio Telescope – WSRT) and spectroheliograms in C IV lines and x-ray emission, obtained on the ultraviolet Spectrometer/Polarimeter (UVSP) and Soft X-Ray Polychromator (XRP) instruments, respectively, on board the Solar Maximum Mission (SMM) satellite.[62] The strong polarized emission at 6 cm and the absence of emission or very weak emission at other wavelengths near sunspot groups, in contrast to a facular region, confirm the correctness of the proposed model with a thin, low-lying transition layer and the absence of plasma with $T > 2 \cdot 10^6$ °K above sunspots.

An adequate quantitative model with T(z) and $n_e(z)$ above the upper limit of our original model (T = 40,000°K, see Sec. 2) can be obtained under the following assumptions: 1) hydrostatic equilibrium; 2) a constant heat-conduction flux F_c in the transition region (see Ref. 63) or $p_e = \text{const}$ instead of $F_c = \text{const}$. The values of p_e and dT/dz for different values of T were obtained in Ref. 41 under the assumption that the filling factor β equals 1.0 for EUV emission. If we take a lower value of β, such as $\beta = 0.1$, the value of p_e hardly changes (it is obtained from the ratio of intensities of lines which are formed at almost the same temperature), while dT/dz and hence F_c are decreased by an order of magnitude in the cool elements from which most of the emission in EUV lines comes and which look like cool "brushes" above the umbra. Then for the rest of the atmospheric volume $\alpha = 1 - \beta$ the assumption of large values of dT/dz and F_c, i.e., a thin and deep-lying transition region, as described above, seems fully demonstrated and consistent with all the available observations.

4. MODEL OF X-RAY EMISSION

The high-resolution x-ray photographs obtained on Skylab show that the stable loops connecting the main sunspots of an active region are the dominant formations in coronal active regions in this spectral range. An example of such loops was studied comprehensively in Ref. 47 (see loops Nos. 2–5 in Fig. 9 in Ref. 47).

It is well known that photographs from Skylab are not very suitable for a study of the temperature structure of an emitting element (see the discussion on pp. 126 and 132 in Ref. 47). Nevertheless, the analysis of photographs from Skylab presented in that paper, from the point of view of the temperature distribution, compels us to assume that: 1) The loop material which can be seen in photographs obtained with a No. 1 filter has a temperature $T = 2.5 \cdot 10^6$ °K (see Fig. 6 in Ref. 47); 2) there is a gradual decline in temperature toward the bases of the loops.

The temperature structure of loops in an active region is investigated with higher accuracy using data of observations in a narrower range. Parkinson[64] used data in the soft x-ray range from OSO 5 on the passage of coronal active regions through the limb, as well as data of rocket spectral observations to investigate the height structure of the regions. He obtained the well-known picture of a loop-shaped structure connecting the main sunspots. In this structure the higher part of the loop between sunspots is the hottest and the temperature gradually decreases toward its base (see Fig. 4 in Ref. 64).

Jakimiec et al.[65] investigated a large, hot, post-flare loop observed on February 10, 1982, using the GSFC spectrometer mounted on board on the OSO 7 satellite. The observations permitted the construction of a map of the temperature distribution on which one can see the gradual temperature decrease along a loop toward its base. The temperature distribution along x-ray loops in an active region is investigated in the present article using the data of Ref. 47.

Not only x-ray photographs from Skylab but also x-ray spectra obtained simultaneously using a rocket spectrometer are presented in that paper. The geometry of x-ray loops in an active region can be established using the high-resolution photographs obtained on Skylab, while the loop temperature structure can be determined on the basis of the x-ray spectra.

As shown in Ref. 47, four x-ray loops connecting the main sunspots of the active region (loops Nos. 2–5 in Fig. 9a in Ref. 47) make the predominant contribution to the recorded x-ray spectra. Since these four loops are very similar to each other in size and x-ray brightness, we investigated some "average" loop, obtained by averaging the four loops. The measured distance between the bases of the loop is $1.12 \cdot 10^5$ km and the height of the loop is $3 \cdot 10^4$ km by our estimates; it is assumed that the loop emits 1/4 of the flux recorded in each of the six investigated x-ray lines (Table I from Ref. 47).

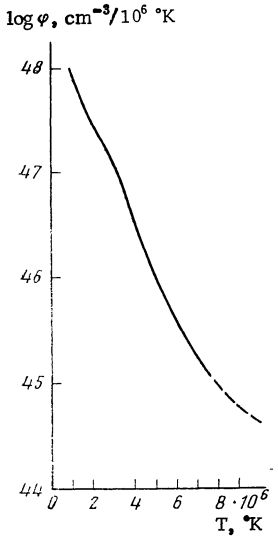

FIG. 2. Distribution of the differential emission measure φ, $cm^{-3}/10^6$ °K, in a typical x-ray loop in an active region based on data of Ref. 47.

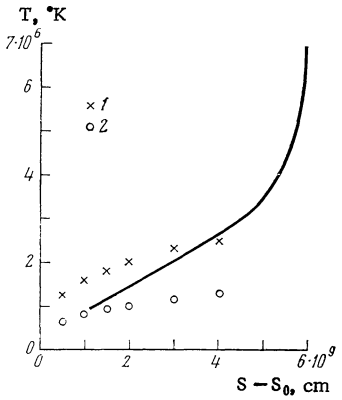

FIG. 3. Temperature distribution along an x-ray loop in an active region, s is the coordinate along the loop and s_0 lies at the base of the loop. The empirical model of a typical loop based on the observations of Ref. 47 is shown by a solid line. Theoretical models of loops in an active region[52] are shown by points. Models for the following values of the gas pressure are shown: 1) for $p = 10^{-5}$ N/cm²; 2) for $p = 10^{-6}$ N/cm².

Starting from the intensities of these lines, we calculated the differential emission measure $\varphi(T)$ for the average loop. The calculations were made using Withbroe's iteration method modified.[66] The results of the $\varphi(T)$ distribution are presented in Fig. 2.

Further, following Ref. 67, we adopted the assumption that temperature variations are significant only along the loops, i.e., that the temperature can be treated as a function only of s, when s is the coordinate along the loop axis. The definition of $\varphi(T)$ can be written as $\varphi(T)dT = n_e^2 dV$, where n_e is the electron density while dV is the volume of plasma with a temperature of from T to T + dT.

Introducing the gas pressure $p = 2n_e kT$ and writing $dV = A(s)ds$, where A(s) is the cross section of the investigated tube, we obtain the equation

$$\frac{dT}{ds} = \left(\frac{p}{2kT}\right)^2 A(s)\frac{1}{\varphi(T)}.$$

Taking p = const and A = const for simplicity, and integrating this equation, we obtain the temperature distribution function T(s) shown in Fig. 3 (solid line). The temperature distributions for theoretical steady-state models (ρ = const) of magnetic tubes[52] are also presented in Fig. 3 for comparison.

It is seen from Fig. 3 that the temperature gradients at the bases of loops actually must be low so that the temperature in the lower part of the loop, up to heights of several tens of thousands of kilometers, not exceed $2 \cdot 10^6$ °K, as is assumed in our model.

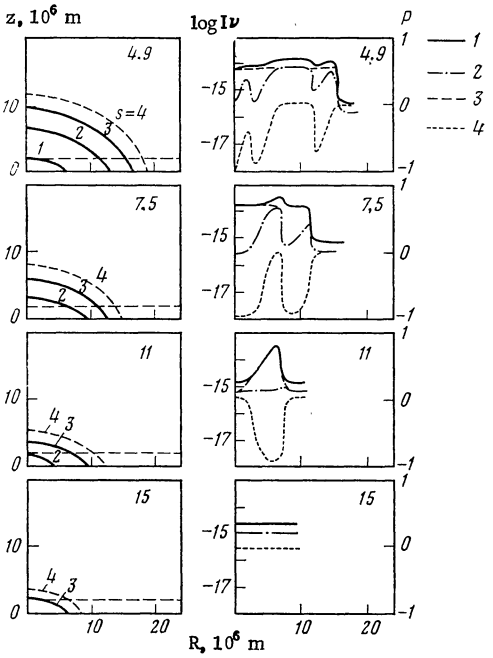

FIG. 4. Distributions of intensity and polarization (right) of the S component (a magnetic dipole located $1.5 \cdot 10^7$ m below the photosphere, B_{max} = 2500 G in the photosphere, n_e and T are indicated in Fig. 1) and positions of gyroresonance levels (left): 1) total intensity; 2) ordinary wave; 3) extraordinary wave; 4) degree of polarization. Frequencies in GHz are given in the upper right corner of each figure.

5. MODELING THE S COMPONENT OF THE RADIO EMISSION

The microwave emission of active regions (the S component) can be considered as an independent opportunity for testing the proposed model at different height levels. For this purpose we constructed an emission model of the S component, which is described in detail in Ref. 68. Earlier models have been described by a whole series of authors (e.g., Refs. 69 and 49).

The present model allows one to calculate the brightness distribution in local sources of the S component at any given fixed frequency. Calculations are made for both magnetoionic wave modes by solving the radiative-transfer equation along the ray trajectory, which yields information about such characteristics as the total flux and the polarization. Thermal bremsstrahlung and gyromagnetic emission are taken into account.

The initial quantities for the numerical calculations are the three-dimensional fields of temperature, electron density, and the magnetic vector. As the first step we assumed axial symmetry; the temperature and density are indicated in Fig. 1 and are extrapolated to greater heights

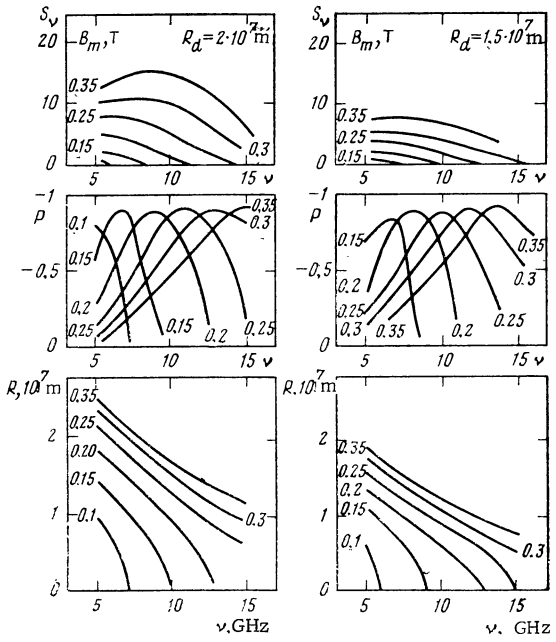

FIG. 5. Spectra of flux density S_ν (top) and degree of polarization p (middle) and effective radii R of the source for different adopted values of B_{max} in teslas and depths R_d of the magnetic dipole (other conditions same as for Fig. 4).

by assuming hydrostatic equilibrium and constancy of the heat-conduction flux F_c. Here F_c or the thickness of the transition layer remains the only free parameter (see Ref. 63 and Sec. 3 above).

Calculated cross sections of brightness and degree of polarization above a sunspot umbra for different frequencies (in our case these are the working frequencies of the RATAN-600 and VLA radio telescopes) are presented in Fig. 4 as an example. The magnetic field model used here consists of one pole of a magnetic dipole. The field essentially depends on two parameters: the maximum strength B_{max} at the center of the base of the source under consideration (R = 0) and the geometrical scale of field decrease. Since the resultant emission depends strongly on the actual magnetic field distribution, we made a whole series of trial calculations with different magnetic field parameters, simulating solar activity at different stages of its development. The resulting spectra of flux density and degree of polarization for different values of B_{max} and for two characteristic scale heights, which are an effective means of diagnostics for regular sunspot groups, are shown in Fig. 5.

Although detailed comparisons with observational results are still a thing of the future, the general tendency outlined on the basis of the calculations is promising. In particular, the lower boundary of the corona at heights on the order of 2000 km above the photosphere is capable of explaining a whole series of observational results discussed above. In the frequency range under consideration the content of cool material, based on observational data on the fine structure in EUV and H α, scarcely exceeds 10%, and therefore it was not taken into account in the tentative calculations of the radio model.

The first applications of our microwave emission model went to explain observations on the RATAN-600 and measurements in the millimeter range.[70,71] The preliminary results are connected with the determination of the scale height of the magnetic field above a sunspot umbra and the degree of inhomogeneity of the facular structure in observations in the millimeter range. As the next step it is proposed to use force-free extrapolation of the magnetic field based on actual magnetograms of concrete AR.

6. CONCLUSIONS

The sunspot model being offered consists of several parts, which must be treated jointly: 1) the umbra model, describing the spatial distributions of thermodynamic quantities up to the transition region on the basis of optical and EUV observations; 2) the magnetic field model; 3) the x-ray emission model; 4) the S-component model.

Preliminary estimates of the emission in various wavelength ranges showed that the model under discussion is capable of explaining the main data of present-day observations. Of course, this conclusion demands further confirmation using more precise model calculations, starting with calculations of the EUV, x-ray, and radio emission. Moreover, the force-free extrapolation of actual magnetic measurements must be used to improve the magnetic field model. Finally, the analysis must be expanded to the entire active region, including faculae and coronal loops. Several steps in this direction are already being made.

Semiempirical working models are required for the study of other physical processes in sunspots, e.g., for the analysis of the propagation and dissipation of magnetohydrodynamic waves and oscillations. Such work was carried out in Ref. 35 using our model.

For the verification and improvement of this model it would be extremely desirable to have improved data on active regions including large sunspots. Such data should have a high spatial resolution in several wavelength ranges at once, from radio to x-ray (to eliminate uncertainties connected with individual differences between sunspots). Coordinated observations, including microwave observations on such large radio telescopes as the RATAN, VLA, and WSRT, EUV, and x-ray observations, as well as ground-based measurements of the magnetic field could provide the required information.

V. N. Obridko, A. Krüger, and J. Staude thank Wroclaw University for the welcome and their Wroclaw colleagues, especially M. and J. Jakimiec, for hospitality during the conference in 1979, at which this work was begun. F. Chiuder-Drago kindly sent us copies of observational data on AR 2490 of June 10, 1980. Completion of this paper was greatly facilitated by the participation of the authors at the working conference on the SMY, which was held at the Crimean Astrophysical Observation (USSR) with the support of the Scientific Committee on Solar–Terrestrial Physics of the International Council of Scientific Unions and the USSR Academy of Sciences.

The participants of the working conference in 1981 wish to thank colleagues at the observatory of Ondřejov, especially V. Bumba, M. Kopecky, and P. Ambroz for their hospitality.

[1]G. Bromboszcz, J. Jakimiec, M. Siarkowski, et al., Proceedings of the 10th Consultation on Solar Physics, Potsdam, 1980, Phys. Solariterr. 16, 155 (1981).

[2]G. Bromboszcz, J. Jakimiec, M. Siarkowski, et al., Proceedings of Solar Maximum Year Workshop, Crimea, Vol. 1 (1981), p. 224.
[3]G. Bromboszcz, J. Jakimiec, M. Siarkowski, et al., Preprint No. 11a, Institute of Terrestrial Magnetism, the Ionosphere, and Radio-Wave Propagation, Moscow (1982).
[4]M. A. Livshits, V. N. Obridko, and S. B. Pikel'ner, Astron. Zh. 43, 1135 (1966) [Sov. Astron. 10, 909 (1967)].
[5]P. V. Foukal, M. C. E. Huber, R. W. Noyes, et al., Astrophys. J. 193, L143 (1974).
[6]P. V. Foukal, Sol. Phys. 43, 327 (1975).
[7]P. V. Foukal, Astrophys. J. 210, 575 (1976).
[8]P. V. Foukal, Astrophys. J. 223, 1046 (1978).
[9]R. H. Levine and G. L. Withbroe, Sol. Phys. 51, 83 (1977).
[10]C.-C. Cheng and O. K. Moe, Sol. Phys. 52, 327 (1977).
[11]G. E. Brueckner, J.-D. F. Bartoe, and M. E. Van Hoosier, Proceedings of the November, 1977, OSO-8 Workshop, Boulder, Colo. (1977), p. 380.
[12]K. R. Nicolas, J.-D. F. Bartoe, G. E. Brueckner, and M. E. Van Hoosier, Astrophys. J. 233, 741 (1979).
[13]G. S. Basri, J. L. Linsky, J.-D. F. Bartoe, G. E. Brueckner, and M. E. Van Hoosier, Astrophys. J. 230, 924 (1979).
[14]G. B. Gel'freikh and A. N. Korzhavin, in: Physics of Sunspots, Proceedings of the Eighth Consultative Conference on Solar Physics, Irkutsk [in Russian], Nauka, Moscow (1976), p. 94.
[15]V. N. Obridko, Astron. Zh. 56, 67 (1979) [Sov. Astron. 23, 38 (1979)].
[16]R. Pallavicini, G. S. Vaiana, G. Tofani, and M. Felli, Astrophys. J. 229, 375 (1979).
[17]The Physics of Sunspots, Proceedings of The Sunspot Workshop, July 14-17, 1981, L. E. Cram and J. H. Thomas, eds., Sacramento Peak Observ. (1981).
[18]G. Stellmacher and E. Wiehr, Astron. Astrophys. 45, 69 (1975).
[19]E. A. Baranovskii, Izv. Krym. Astrofiz. Obs. 49, 25 (1974).
[20]E. A. Baranovskii, Izv. Krym. Astrofiz. Obs. 51, 56 (1974).
[21]R. B. Teplitskaya, S. A. Grigor'eva (Grigor'eva) (Efendieva), and V. G. Skochilov, Sol. Phys. 56, 293 (1978).
[22]R. B. Teplitskaya, S. A. Grigor'eva, and V. G. Skochilov, Issled. Geomagn. Aeronom. Fiz. Solntsa 42, 48 (1977).
[23]F. Kneer and W. Mattig, Astron. Astrophys. 65, 17 (1978).
[24]J.-D. F. Bartoe, G. E. Brueckner, K. R. Nicolas, et al., Mon. Not. R. Astron. Soc. 187, 463 (1979).
[25]C. Jordan, J.-D. F. Bartoe, G. E. Brueckner, et al., Mon. Not. R. Astron. Soc. 187, 473 (1979).
[26]C. Jordan, G. E. Brueckner, J.-D. F. Bartoe, et al., Astrophys. J. 226, 687 (1978).
[27]J.-D. F. Bartoe, G. E. Brueckner, G. D. Sandlin, and M. E. Van Hoosier, Astrophys. J. 223, L51 (1978).
[28]F. Kneer, G. Scharmer, W. Mattig, et al., Sol. Phys. 69, 289 (1981).
[29]T. R. Ayres and J. L. Linsky, Astrophys. J. 205, 874 (1976).
[30]J. Staude, Bull. Astron. Inst. Czech. 27, 365 (1976).
[31]J. Staude, Bull. Astron. Inst. Czech. 29, 71 (1978).
[32]P. Maltby, Sol. Phys. 55, 335 (1977).
[33]J. Staude, Astron. Astrophys. 100, 284 (1981).
[34]J. Staude, Phys. Solariterr. 14, 58 (1980).
[35]Yu. D. Zhugzhda (J. D. Zugzda), V. Lacans, and J. Staude, Sol. Phys. 82, 369 (1983).
[36]J. Staude, HHI-STP Report No. 14, Zentralinstitut für Solar-Terrestrische Physik, Berlin (1983).
[37]B. W. Lites and A. Skumanich, Astrophys. J., Suppl. Ser. 49, 293 (1982).
[38]E. H. Avrett, in: The Physics of Sunspots, Proceedings of the Sunspot Workshop, July 14-17, 1981, L. E. Cram and J. H. Thomas, eds., Sacramento Peak Obs. (1981), p. 235.
[39]H. S. Yun, H. A. Beebe, and W. E. Baggett, in: The Physics of Sunspots, Proceedings of the Sunspot Workshop, July 14-17, 1981, L. E. Cram and J. H. Thomas, eds., Sacramento Peak Obs. (1981), p. 142.
[40]H. A. Beebe, W. E. Baggett, and H. S. Yun, Sol. Phys. 79, 31 (1982).
[41]K. R. Nicolas, M. O. Kjeldseth, J.-D. F. Bartoe, and G. E. Brueckner, Sol. Phys. 81, 253 (1982).
[42]M. R. Kundu, E. J. Schmahl, and M. Gerassimenko, Astron. Astrophys. 82, 265 (1980).
[43]N. Seehafer and J. Staude, Astron. Nachr. 300, 151 (1979).
[44]N. Seehafer and J. Staude, Sol. Phys. 67, 121 (1980).
[45]M. Felli, K. R. Lang, and R. F. Willson, Astrophys. J. 247, 325 (1981).
[46]E. J. Schmahl, M. R. Kundu, K. T. Strong, et al., Sol. Phys. 80, 233 (1982).
[47]J. P. Pye, K. D. Evans, R. J. Hutcheon, et al., Astron. Astrophys. 65, 123 (1978).
[48]G. B. Gel'freikh and B. I. Lubyshev, Astron. Zh. 56, 562 (1979) [Sov. Astron. 23, 316 (1979)].
[49]E. Ya. Zlotnik, Astron. Zh. 45, 310, 585 (1968) [Sov. Astron. 12, 245, 464 (1968)].
[50]C. E. Alissandrakis and M. R. Kundu, Astrophys. J. 253, L49 (1982).
[51]K. R. Lang and R. F. Willson, Astrophys. J. 255, L111 (1982).
[52]R. Rosner, W. H. Tucker, and G. S. Vaiana, Astrophys. J. 220, 643 (1978).
[53]J. F. Vesecky, S. K. Antiochos, and J. H. Underwood, Astrophys. J. 233, 987 (1979).
[54]P. Maltby, Sol. Phys. 43, 91 (1975).
[55]R. Pallavicini, T. Sakurai, and G. S. Vaiana, Astron. Astrophys. 98, 316 (1981).
[56]K. P. Dere, J.-D. F. Bartoe, and G. E. Brueckner, Astrophys. J. 259, 366 (1982).
[57]K. P. Dere, J.-D. F. Bartoe, and G. E. Brueckner, Astrophys. J. 259, 366 (1982).
[58]A. E. Kingston, J. G. Doyle, P. L. Dufton, and J. B. Gurman, Sol. Phys. 81, 47 (1982).
[59]W. Henze, Jr., E. Tandberg-Hannssen, M. J. Hagyard, et al., Sol. Phys. 81, 231 (1982).
[60]K. R. Lang, R. F. Willson, and V. Gaizauskas, Astrophys. J. 267, 455 (1983).
[61]N. Seehafer, Sol. Phys. 81, 69 (1982).
[62]F. Chiuder-Drago, R. Bandiera, R. Falciani, et al., Sol. Phys. 80, 71 (1982).
[63]C. E. Alissandrakis, M. R. Kundu, and P. Lantos, Astron. Astrophys. 82, 30 (1980).
[64]J. H. Parkinson, Sol. Phys. 28, 487 (1973).
[65]J. Jakimiec, W. M. Neupert, B. Sylwester, and J. Sylwester, Report at the Ninth Consultation on Solar Physics, Wroclaw (1978).
[66]J. Sylwester, J. Schrijver, and R. Mewe, Sol. Phys. 67, 285 (1980).
[67]G. L. Withbroe, Astrophys. J. 225, 641 (1978).
[68]A. Krüger, F. Fürstenberg, J. Hildebrandt, and J. Staude, HHI-STP Report No. 14, Zentralinstitut fur Solar-Terrestrische Physik, Berlin (1983).
[69]P. Lantos, Ann. Astrophys. 31, 105 (1968).
[70]Sh. B. Akhmedov, G. B. Gel'freikh, A. Kruger, F. Furstenberg, and J. Hildebrandt, Soln. Dannye 10, 72 (1982).
[71]S. Urpo, J. Hildebrandt, K. Pflug, et al., Phys. Solariterr., No. 19, 5 (1982).

Translated by Edward U. Oldham